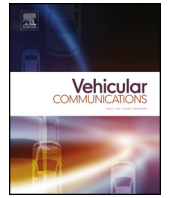




Contents lists available at ScienceDirect

Vehicular Communications

www.elsevier.com/locate/vehcom



Performance analysis of vehicle-to-vehicle communication with full-duplex amplify-and-forward relay over double-Rayleigh fading channels

Ba Cao Nguyen^a, Tran Manh Hoang^a, Le The Dung^{b,c,*}, 1

^a Faculty of Radio Electronics, Le Quy Don Technical University, Viet Nam

^b Division of Computational Physics, Institute for Computational Science, Ton Duc Thang University, Ho Chi Minh City, Viet Nam

^c Faculty of Electrical and Electronics Engineering, Ton Duc Thang University, Ho Chi Minh City, Viet Nam

ARTICLE INFO

Article history:

Received 1 March 2019

Received in revised form 17 June 2019

Accepted 3 July 2019

Available online xxx

Keywords:

Vehicle-to-vehicle communication

Full-duplex

Self-interference cancellation

Amplify-and-forward

Outage probability

Symbol error rate

ABSTRACT

In this paper, we investigate a vehicle-to-vehicle (V2V) communication system where a full-duplex (FD) relay uses amplify-and-forward (AF) protocol. We consider two cases for the AF protocol, i.e. fixed and variable gain relaying. Furthermore, the channels between the nodes are considered as the double (cascaded) Rayleigh fading distributions. We derive the closed-form expressions for the outage probabilities (OPs) and symbol error rates (SERs) in these two cases. The numerical results show the impact of the double Rayleigh fading channels on the system performance in comparison with this system over Rayleigh fading channels. Moreover, the effects of the distances, path loss exponent, and residual self-interference (RSI) on the system performance are also studied. We find that for a given transmission power of the nodes in the system, there are optimal distances for the cases of fixed and variable gain which provide the best system performance. All analysis results in this paper are validated by Monte-Carlo simulation results.

© 2019 Elsevier Inc. All rights reserved.

1. Introduction

In the age of digital technology, almost personal devices are connected to the Internet to exchange data. Not only connect the people in voice and video, smart devices are connected to the others to control many operations such as in smart home, intelligent transportation systems (ITS). Recently, device-to-device (D2D) communication is fast developed, leading to the demand of big data for the wireless communication such as the Internet of Things (IoT), the fifth generation (5G) of mobile communications. To resolve the problem of limited spectrum in wireless networks, various methods have been proposed such as massive multiple-input multiple-output (MIMO), full-duplex (FD), non-orthogonal multiple access (NOMA) [1–3].

Among these methods, the FD communication has become a hot topic due to the fact that the FD devices can transmit and receive the signal at the same time and on the same frequency band,

that leads to the capability of doubling the theory capacity. With the development of antenna design techniques and the analog and digital signal processing, the operation of the FD devices is experimented when the self-interference cancellation (SIC) is suppressed up to 110 dB in both theories and experiments [4,5]. Therefore, the FD communication is a promising solution for the future wireless networks and the researches on the FD system are conducted in many aspects such as the SIC techniques [5–7], the performance analysis in terms of the outage probability (OP), and the ergodic capacity [3,8–11].

In the literature, due to the benefits of using relay node in wireless systems, such as enhancing the reliability, coverage, and the performance of wireless systems [12,13], many researches have analyzed the relay systems where the FD relay is used to improve the spectral efficiency [3,8,10,14,15]. Their results showed that the system with FD relay can be applied in the realistic scenarios where various SIC are conducted to suppress the self-interference. In these studies, the OP, symbol error rate (SER), and the ergodic capacity were analyzed in the case of imperfect SIC at FD relay node. The authors demonstrated that the FD systems can nearly double the spectrum when the RSI is very small. In addition, the OP and SER of these systems reach the error floor due to the RSI. Furthermore, the optimal power allocation scheme for the FD

* Corresponding author at: Division of Computational Physics, Institute for Computational Science, Ton Duc Thang University, Ho Chi Minh City, Viet Nam.

E-mail addresses: bacao.sqt@gmail.com (B.C. Nguyen), tranmanhhoang@tcu.edu.vn (T.M. Hoang), lethedung@tdtu.edu.vn (L.T. Dung).

¹ Member IEEE.

mode was proposed to reduce the impact of the RSI and improve the system performance [9,15].

Today, vehicular communications play an important role due to their applications in autonomous vehicles [16–20]. On the other hand, almost people control the system through the smart devices even when these devices move on the road, which form the vehicle-to-vehicle (V2V) communication. Furthermore, the channels between the devices in V2V communication exhibit double Rayleigh fading, thus they are worse than the channels in traditional wireless systems where the channels between the devices are usually characterized by Rayleigh fading. Therefore, the system performance of V2V communication will be decreased in comparison with one over Rayleigh fading channel. However, due to the fact that the V2V communication can be applied for the intelligent transportation systems (ITS) [19,20], it is vitally necessary to analyze and improve the system performance. Since they provide many applications for the traffic safety and efficiency, a lot of researches have focused on the applications, architectures, protocols, and channel models of V2V communications.

Particularly, in V2V communication systems, since all nodes are vehicles, the channel models which are usually used for wireless systems such as Rayleigh, Rician or Nakagami- m do not fit for almost V2V channel measurements [21–23]. It is because those channels are often applied for stationary communication links, where all nodes are fixed. On the other hand, the theoretical analysis and field measurement [21–23] demonstrated that the double Rayleigh fading distribution can precisely characterize the V2V channel, because two-bounce scattering components caused by scatterers around both the transmitter's and receiver's local environments will generate a cascaded (double) Rayleigh fading distribution [22]. Furthermore, the double Rayleigh fading distribution also fits for various scenarios such as suburban outdoor-to-indoor mobile-to-mobile communication scenarios or keyhole channels [24].

The impact of double Rayleigh fading channels on the V2V communication systems has been analyzed in several works in the literature [18,20,25–28]. Their results demonstrated that the double Rayleigh fading channels reduce the system performance strongly in both theory and experiments. Additionally, based on the theoretical analysis and field measurement [21–24], the double Rayleigh fading channels can be applied for various scenarios such as urban, suburban and forest environments in V2V communication systems. The system performance of V2V communication in the case of point-to-point HD devices over double Rayleigh fading channels was analyzed in [20,29]. Recently, the combination of the FD technique with V2V communication in a system has been conducted, such as in [19,30–32]. The work in [19] considered the potential of FD technique in V2V communication. The advantages and disadvantages of the FD-V2V communication was analyzed. In addition, the guideline for the design and the deployment of medium access control was also proposed. Furthermore, the results in [30] demonstrated that a FD vehicle can detect collision and apply this ability in cooperative automated driving. On the other hand, the antenna design is very important for the FD communication, thus [31] proposed a novel dual-band full-duplex antenna array for FD-V2V communication. In this antenna array, the authors used two ports to increase the isolation between the transmitted signal and received signal, resulting in the decreased self-interference. Furthermore the size, weight, and cost of the antenna array is reduced because the authors combined the filtering, duplexing, and radiation in a single device. In [32], the FD vehicular access networks without the channel state information (CSI) at transmitter was investigated. The optimal blind interference alignment scheme was proposed to improve the sum rate of the system.

Although the FD-V2V communication has been studied, however the researches on this system are limited. It is because when

two techniques are combined in a system, the system performance will be decreased due to the impacts of the RSI in FD mode and the double Rayleigh fading channels. Furthermore, the channels in V2V communications are considered as double Rayleigh fading channels that leads to the computation complexity. Therefore, the studies on FD-V2V communications have just archived some certain results. All previous works did not derive mathematical expressions for analyzing the OP and SER. Motivated by this issue, in this paper, we propose the novel model which combines the FD and V2V in a system. In this system, the source node which operates in half-duplex (HD) mode transmits the signal to the destination node via the relay node which operates in FD mode. The relay node uses amplify-and-forward (AF) protocol with fixed and variable gain relaying.

The contributions of this paper can be summarized as follows:

- We consider the FD relay system where all nodes are vehicles that form the FD-V2V communication system. At the FD relay node, we investigate two cases: fixed and variable gain relaying with imperfect SIC. The channels between nodes are considered as the double Rayleigh fading channels.

- We successfully derive the exact expressions of the OP and SER in the case of imperfect SIC at the FD relay node for fixed and variable gain relaying. Based on these expressions, the system throughput is also investigated.

- We show that the system performance in both cases fixed and variable gain relaying are decreased strongly compared with the system over Rayleigh fading channel. Furthermore, the system performance is significantly affected by the RSI due to the FD mode. On the other hand, the impacts of far distance between the vehicles and the path loss exponent are also investigated. We observe that there is an optimal distance between three nodes which provides the best system performance for two cases of gain relaying and the optimal distance of the fixed gain is different with that of the variable gain. Finally, the Monte-Carlo simulations are used to verify the correctness of the analysis results.

The rest of this paper is organized as follows. Section 2 describes the signal and system models, while Section 3 presents the analysis of system performance in terms of the OP and SER. Section 4 gives the numerical results and discussions. Finally, Section 5 concludes the paper.

2. System model

In this section, the signal and system models of a FD-V2V communication system is described. As illustrated in Fig. 1, the signal is transmitted from a source node (S) to a destination node (D) via a relay node (R). In this system, R operates in FD mode with two antennas, one for transmitting and the other for receiving. Meanwhile, S and D operate in the HD mode with single antenna. We should note that in practical system, the R can use one shared-antenna for both transmitting and receiving by using the circulator to separate the transmitted and received signal. However, using two separate antennas can easily apply various SIC techniques for FD mode, such as the isolation, the analog and digital cancellations [4,33]. Therefore, in this paper, we assume that the relay uses two separate antennas to obtain good SIC capability.

On the other hand, the relay uses AF protocol. We investigate two cases at the relay node. Specifically, when the relay node knows the instantaneous channel gain from the source node to the relay node, it uses variable-gain relaying. Otherwise, it uses fixed-gain relaying. Furthermore, all nodes in the system are mobile nodes which form a V2V communication system. Therefore, the channel between the source and the relay, the relay and the destination are considered as the double Rayleigh channels. In this case, all channels in the system are independent and identically distributed (IID) double Rayleigh random variables (RVs).

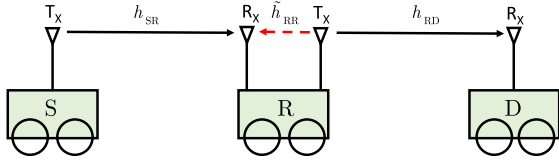


Fig. 1. System model of the V2V communication system with FD relay. (For interpretation of the colors in the figure(s), the reader is referred to the web version of this article.)

At the time slot t , R receives signal from S. This received signal can be expressed as

$$y_R = \sqrt{d_{SR}^{-\alpha} P_S} h_{SR} x_S + \tilde{h}_{RR} \sqrt{d_{RR}^{-\alpha} P_R} x_R + n_R, \quad (1)$$

where d_{SR} and d_{RR} are the distances between S and R and between the transmission antenna and reception antenna of R, respectively; α is the path loss exponent and its value ranges from 2 to 6; h_{SR} and \tilde{h}_{RR} are respectively the fading coefficients of the channels from S to R and from the transmitting to the receiving antennas of R; x_S and x_R represent the complex signals which are transmitted from S and R, respectively; n_R is the Additive White Gaussian Noise (AWGN) with zero-mean and variance of σ^2 , i.e. $n_R \sim \mathcal{CN}(0, \sigma^2)$. It is also noted that, in the literature such as [34], the interference between vehicles can be utilized in various applications such as energy harvesting, channel estimation, message flooding, link security and signal alignment. However, in this scenario the SI signal is not a useful signal and the relay must suppress it to improve the system performance.

As aforementioned, the relay node can combine all SIC techniques [5,6,33,35]. However, due to the imperfect SIC, the residual self-interference (RSI) still strongly impacts the system performance. Specifically, after applying all SIC techniques, the RSI, denoted by I_R , can be modeled as the Gaussian distribution [5,6,33] with zero mean and variance of γ_{RSI} , which is well-fitted with the measurement and experiment results [4,8–10]. On the other hand, this assumption helps us reduce the variables in mathematical expressions because when we consider I_R is the Gaussian variable, its variance is a constant. It is noted that $\gamma_{RSI} = \tilde{\Omega} P_R$ where $\tilde{\Omega}$ refers to the SIC capability of the FD node. Therefore, the received signal at R after SIC can be rewritten as

$$y_R = \sqrt{d_{SR}^{-\alpha} P_S} h_{SR} x_S + I_R + n_R. \quad (2)$$

Due to the AF scheme, the transmitted signal at the R is its previous received signal after amplifying, that means $x_R = G y_R$, where G is the relaying gain which is subjected to the normalized transmission power of the relay. Furthermore, because of the double Rayleigh channels, h_{SR} is the multiplication of two independent Rayleigh variables g_1 and g_2 , i.e. $h_{SR} = g_1 g_2$. Therefore, the fixed gain (G_f) and the variable gain (G_v) corresponding to the channel conditions are calculated as

$$G_f \triangleq \sqrt{\frac{1}{d_{SR}^{-\alpha} \Omega_1 \Omega_2 P_S + \gamma_{RSI} + \sigma^2}}, \quad (3)$$

$$G_v \triangleq \sqrt{\frac{1}{d_{SR}^{-\alpha} \rho_1 \rho_2 P_S + \gamma_{RSI} + \sigma^2}}, \quad (4)$$

where $\rho_1 = |g_1|^2$ and $\rho_2 = |g_2|^2$ are the instantaneous channel gains, $\Omega_1 = \mathbb{E}\{\rho_1\}$, $\Omega_2 = \mathbb{E}\{\rho_2\}$, $\mathbb{E}\{\cdot\}$ denotes the expectation operator.

According to the FD mode, the relay forwards the signal to the destination after amplifying this signal at the same time and on

the same frequency band. Therefore, the received signal at D is given by

$$y_D = \sqrt{d_{RD}^{-\alpha} P_R} h_{RD} x_R + n_D, \quad (5)$$

where d_{RD} is the distance between R and D; h_{RD} is the fading coefficient of R–D link; n_D is the AWGN at the destination D, $n_D \sim \mathcal{CN}(0, \sigma^2)$. It is also noted that h_{RD} has the same distribution with h_{SR} , that means $h_{RD} = g_3 g_4$, where g_3 and g_4 are two independent Rayleigh variables. Substituting x_R by $G y_R$, we have

$$y_D = \sqrt{d_{RD}^{-\alpha} P_R} h_{RD} G (\sqrt{d_{SR}^{-\alpha} P_S} h_{SR} x_S + I_R + n_R) + n_D. \quad (6)$$

From (6), the end-to-end signal-to-interference-plus-noise ratio (SINR) for the cases of fixed and variable gains are computed as

$$\begin{aligned} \gamma_f &= \frac{(d_{SR} d_{RD})^{-\alpha} P_S P_R |h_{SR}|^2 |h_{RD}|^2}{d_{RD}^{-\alpha} P_R |h_{RD}|^2 (\gamma_{RSI} + \sigma^2) + \sigma^2 / G_f^2} \\ &= \frac{(d_{SR} d_{RD})^{-\alpha} P_S P_R \rho_1 \rho_2 \rho_3 \rho_4}{d_{RD}^{-\alpha} P_R \rho_3 \rho_4 (\gamma_{RSI} + \sigma^2) + \sigma^2 / G_f^2}, \end{aligned} \quad (7)$$

$$\gamma_v = \frac{(d_{SR} d_{RD})^{-\alpha} P_S P_R \rho_1 \rho_2 \rho_3 \rho_4}{d_{RD}^{-\alpha} P_R \rho_3 \rho_4 (\gamma_{RSI} + \sigma^2) + \sigma^2 (d_{SR}^{-\alpha} P_S \rho_1 \rho_2 + \gamma_{RSI} + \sigma^2)}, \quad (8)$$

where $\rho_3 = |g_3|^2$ and $\rho_4 = |g_4|^2$.

3. System performance

3.1. Outage probability

The OP of the considered system is defined as the probability that the transmission rate of the system is less than a given data rate. We assume that the minimum required data rate of the system is \mathcal{R} (bit/s/Hz), thus the OP is calculated as

$$P_{\text{out}} = \Pr\{\log_2(1 + \gamma) < \mathcal{R}\} = \Pr\{\gamma < 2^{\mathcal{R}} - 1\}, \quad (9)$$

where γ is the SINR of the considered system which is determined by (7) for the case of fixed gain relaying and by (8) for the case of variable gain relaying. Let $x = 2^{\mathcal{R}} - 1$ be the threshold for the OP, then (9) becomes

$$P_{\text{out}} = \Pr\{\gamma < x\}. \quad (10)$$

Theorem 1. The OPs of the FD relay system over double Rayleigh fading channels and under the impact of the RSI in the cases of fixed gain (P_{out}^f) and variable gain (P_{out}^v) are expressed as follows

$$\begin{aligned} P_{\text{out}}^f &= 1 - \frac{\pi C_f}{2M} \sum_{m=1}^M \frac{\sqrt{1 - \phi_m^2}}{z} \sqrt{\frac{A_f x}{-\ln z} + B_f x} \\ &\quad \times K_0(\sqrt{-2C_f \ln z}) K_1\left(\sqrt{\frac{A_f x}{-\ln z} + B_f x}\right), \end{aligned} \quad (11)$$

$$\begin{aligned} P_{\text{out}}^v &= 1 - \frac{\pi C_v}{2M} \sum_{m=1}^M \frac{\sqrt{1 - \phi_m^2}}{z} \sqrt{\frac{A_v (x^2 + x)}{-\ln z} + B_v x} \\ &\quad \times K_0(\sqrt{-2C_v \ln z + D_v x}) K_1\left(\sqrt{\frac{A_v (x^2 + x)}{-\ln z} + B_v x}\right), \end{aligned} \quad (12)$$

where

$$A_f = \frac{4\sigma^2}{(d_{SR}d_{RD})^{-\alpha}\Omega_1\Omega_2P_S P_R G_f^2}; B_f = \frac{4(\gamma_{RSI} + \sigma^2)}{d_{SR}^{-\alpha}\Omega_1\Omega_2P_S};$$

$$C_f = \frac{2}{\Omega_3\Omega_4}; A_v = \frac{4\sigma^2(\gamma_{RSI} + \sigma^2)}{(d_{SR}d_{RD})^{-\alpha}\Omega_1\Omega_2P_S P_R};$$

$$B_v = B_f; C_v = C_f; D_v = \frac{4\sigma^2}{d_{RD}^{-\alpha}\Omega_3\Omega_4P_R}$$

$$z = \frac{1}{2} + \frac{1}{2}\phi_m; \phi_m = \cos\left(\frac{(2m-1)\pi}{2M}\right);$$

$\Omega_i = \mathbb{E}\{\rho_i\}$ is the average channel gain of link i , $i = 1, 2, 3, 4$; M is the complexity-accuracy trade-off parameter; $K_0(\cdot)$ and $K_1(\cdot)$ denote the zero and the first-order modified Bessel function of the second kind, respectively.

Proof. The detailed proof is presented in Appendix A. \square

3.2. Symbol error rate

The SER of the wireless system is calculated from the following expression [36]

$$SER = a\mathbb{E}\{Q(\sqrt{b\gamma})\} = \frac{a}{\sqrt{2\pi}} \int_0^\infty F\left(\frac{t^2}{b}\right) e^{-\frac{t^2}{2}} dt, \quad (13)$$

where a and b are constants and their values depend on the modulation types [36], e.g. $a = 2, b = 1$ for quadrature phase shift keying (QPSK) and 4-quadrature amplitude modulation (4-QAM), $a = 1, b = 2$ for the binary phase-shift keying (BPSK) modulation;

$Q(x) = \frac{1}{\sqrt{2\pi}} \int_x^\infty e^{-t^2/2} dt$ is the Gaussian function; γ and $F(\cdot)$ are respectively the end-to-end SINR and its CDF. It is noted that from the definition of the CDF and the OP, we can replace $F(x)$ by the P_{out} of the system which are specified in (11) and (12).

Theorem 2. The SERs in the cases of fixed gain relaying (SER_f) and variable gain relaying (SER_v) of the system are obtained as follows

$$SER_f = \frac{a\sqrt{b}}{2\sqrt{2\pi}} \left[\sqrt{\frac{2\pi}{b}} - \frac{\pi C_f}{2M} \sum_{m=1}^M \frac{\sqrt{1-\phi_m^2}}{z} \sqrt{\frac{A_f}{-\ln z}} + B_f \right]$$

$$\times K_0(\sqrt{-2C_f \ln z}) \exp\left(\frac{1}{4b} \left(\frac{A_f}{-\ln z} + B_f\right)\right)$$

$$\times \frac{\Gamma(\frac{3}{2})\Gamma(\frac{1}{2})}{\sqrt{\frac{b}{2}(-\ln z + B_f)}} W_{-\frac{1}{2}, \frac{1}{2}}\left(\frac{1}{2b} \left(\frac{A_f}{-\ln z} + B_f\right)\right), \quad (14)$$

$$SER_v = \frac{a\sqrt{b}}{2\sqrt{2\pi}} \left[\sqrt{\frac{2\pi}{b}} - \frac{\pi^2 C_v}{2bMN} \sum_{m=1}^M \sum_{n=1}^N \frac{\sqrt{1-\phi_m^2}}{z} \right]$$

$$\times \sqrt{1-\phi_n^2} \sqrt{\frac{A_v(b-2\ln t)}{-b \ln z}} + B_v$$

$$\times K_0\left(\sqrt{-2C_v \ln z - \frac{2D_v \ln t}{b}}\right)$$

$$\times K_1\left(\sqrt{-\frac{2}{b} \left[\frac{A_v(b-2\ln t)}{-b \ln z} + B_v\right] \ln t}\right), \quad (15)$$

where Γ and W are respectively the Gamma and Whittaker functions [37]; N is the complexity-accuracy trade-off parameter; $t = \frac{1}{2} + \frac{1}{2}\phi_n$; $\phi_n = \cos(\frac{(2n-1)\pi}{2N})$.

Proof. The detailed proof is presented in Appendix B. \square

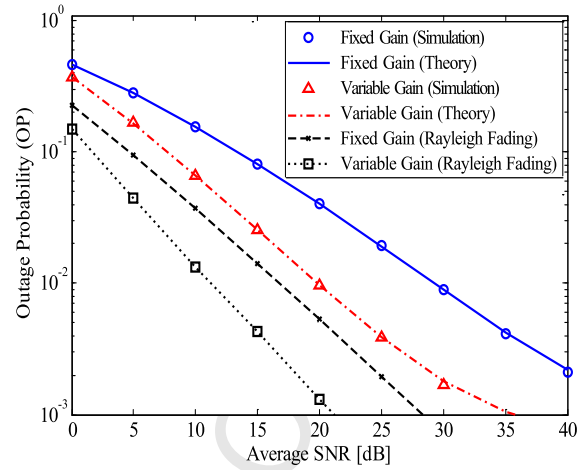


Fig. 2. The OPs of the considered FD-V2V communication system versus the average SNR in comparison with this system over Rayleigh fading channel for $\alpha = 4$, $d_{SR} = d_{RD} = 0.5$, $\tilde{\Omega} = -30$ dB, and $\mathcal{R} = 1$ bit/s/Hz.

4. Numerical results and discussion

In this section, we evaluate the system performance by using the mathematical expressions in Theorems 1 and 2. Furthermore, we also use the Monte-Carlo simulations and plot both the theory and simulation curves on a figure to demonstrate the correctness of the derived mathematical expressions. On the other hand, we investigate the OP and SEP versus the SNR of the system. It is also noted that in this paper the SNR is calculated by the ratio of the transmission power (P_S and P_R) to the variance of AWGN (σ^2), i.e. $SNR = P_S/\sigma^2 = P_R/\sigma^2$. The average channel gains $\Omega_i = 1$ with $i \in \{1, 2, 3, 4\}$. The SIC capability $\tilde{\Omega}$ is varied to evaluate the impact of the RSI on the system performance. The distance d_{SR} and d_{RD} are chosen so that $d_{SR} + d_{RD} = 1$, which is similar to [28,38].

Fig. 2 investigates the OPs of the considered FD-V2V communication system versus the average SNR in the cases of fixed and variable gain relaying in comparison with this system over Rayleigh fading channel. In this figure, we use $d_{SR} = d_{RD} = 0.5$ and $\alpha = 4$. The minimum required data rate $\mathcal{R} = 1$ bit/s/Hz, thus the threshold $x = 2^{\mathcal{R}} - 1 = 1$. The SIC capability $\tilde{\Omega} = -30$ dB. To demonstrate the performance degradation of the system over double Rayleigh fading channels, we also conduct the simulations for this system over Rayleigh fading channel. As shown in the Fig. 2, the analysis results of the expressions in Theorem 1 are matched with the simulation results. This confirms the correctness of the Theorem 1. It is noted that the fixed-gain theory curve is plotted by using (11) while the variable-gain theory curve is plotted by using (12). Furthermore, the variable gain relaying increases the system performance significantly compared with the fixed-gain relaying. Specially at $OP = 10^{-2}$, the variable-gain relaying has approximately 10 dB gain in comparison with the fixed-gain relaying. On the other hand, the system performance in the case of V2V decreases almost 10 dB in comparison with this system over Rayleigh fading channels.

Fig. 3 illustrates the system throughput of the considered FD-V2V communication system with $\alpha = 4$, $d_{SR} = d_{RD} = 0.5$, $\tilde{\Omega} = -30$ dB in comparison with the Rayleigh fading system. Herein, the system throughput is calculated by $\mathcal{T} = \mathcal{R}(1 - P_{out})$. In this figure, we consider two data transmission rates, i.e. $\mathcal{R} = 2$ and $\mathcal{R} = 4$ bit/s/Hz. It is shown that in low SNR regime, the difference between the system throughput of the considered system and that of system over Rayleigh fading channel is significant. At $SNR = 15$ dB and $\mathcal{R} = 4$ bit/s/Hz, the system throughput of considered system is nearly less than 1 bit/s/Hz in comparison with that of the system over Rayleigh fading channel. On the other hand, it is difficult to

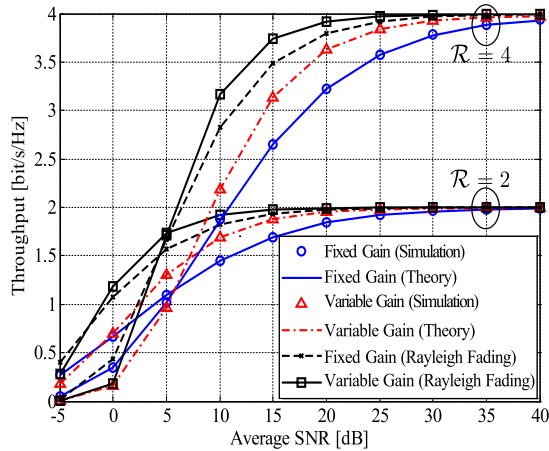


Fig. 3. The system throughput versus the average SNR, $\alpha = 4$, $d_{SR} = d_{RD} = 0.5$, $\tilde{\Omega} = -30$ dB.

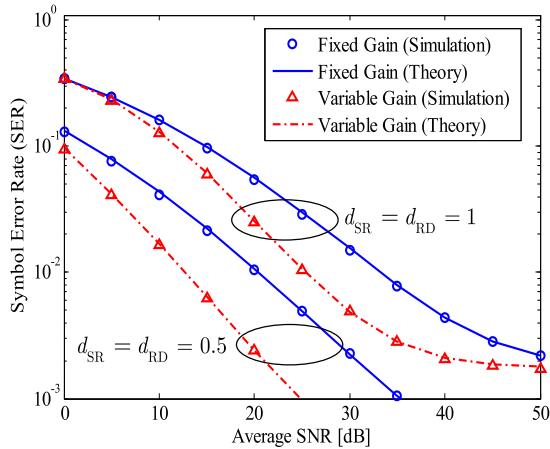


Fig. 4. The SER of the considered FD-V2V communication system using BPSK modulation with $\alpha = 4$, $\tilde{\Omega} = -30$ dB.

reach the transmission target for the considered system, especially with high data transmission rate, i.e. $\mathcal{R} = 4$ bit/s/Hz.

Fig. 4 shows the SER of the considered FD-V2V communication system using BPSK modulation ($a = 1, b = 2$) versus the average SNR with $\alpha = 4$ and $\tilde{\Omega} = -30$ dB. In this figure, we consider two distances, i.e. $d_{SR} = d_{RD} = 1$ and $d_{SR} = d_{RD} = 0.5$. Fig. 4 shows that the theory curves which are plotted by using the Theorem 2 are matched with the simulation ones. In the case of $d_{SR} = d_{RD} = 1$, the SER of variable gain relaying goes down slowly and reaches the error floor at high SNR regime while SER of fixed gain relaying continuously goes down. The reason is that in high SNR regime both fixed and variable gains relaying have the same error floor. Due to the fact that when $\text{SNR} \rightarrow \infty$ the SINRs in (7) and (8) go to constant values. Furthermore, when the distances are decreased, such as for $d_{SR} = d_{RD} = 0.5$, the difference between the fixed and variable gains relaying is increased.

In Fig. 5, we investigate the impact of the path loss exponent on the SER of the considered FD-V2V communication system with $d_{SR} = d_{RD} = 0.5$ and $\tilde{\Omega} = -30$ dB. Due to the fact that the distances (d_{SR}, d_{RD}) are smaller than 1, thus larger α results in better SER of the system. As shown in Fig. 5, both SERs in cases of fixed and variable gain relaying increase significantly when $\alpha = 6$ in comparison with those when $\alpha = 2$. At $\text{SER} = 10^{-2}$, the gains in both cases of fixed and variable gain relaying when $\alpha = 6$ are 10 dB in comparison with those when $\alpha = 2$. Therefore, when the system operates in the environment which has high path loss exponent, it

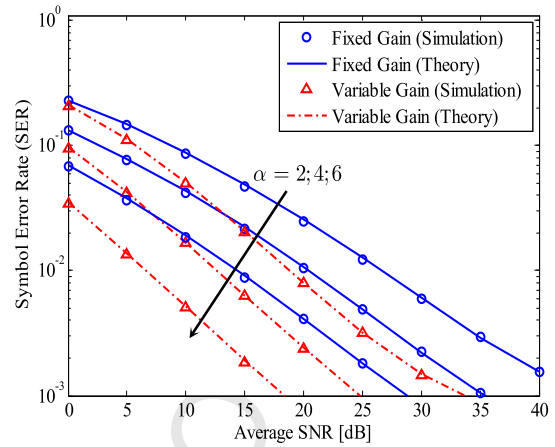


Fig. 5. The impact of the path loss exponent on the SER of the considered FD-V2V communication system versus the average SNR for different path loss exponent, $d_{SR} = d_{RD} = 0.5$ and $\tilde{\Omega} = -30$ dB.

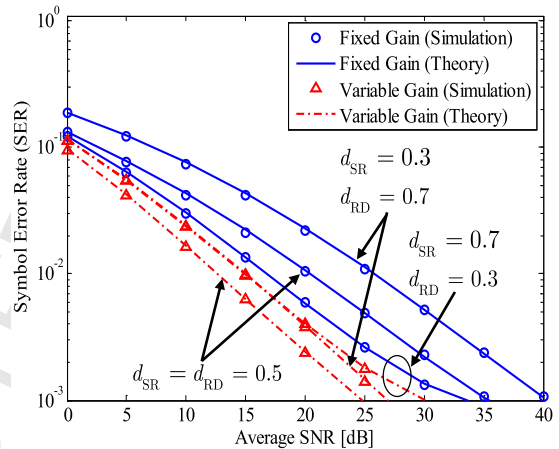


Fig. 6. The SER of the considered FD-V2V communication system versus the average SNR for different settings of the distances among vehicles, $\tilde{\Omega} = -30$ dB.

is necessary to apply various methods such as channel coding, orthogonal frequency division multiplexing (OFDM) to enhance the system performance.

Fig. 6 shows the SER of the FD-V2V communication system versus the average SNR under the impact of the RSI and the distance between vehicles. We consider $d_{SR} + d_{RD} = 1$, $\alpha = 4$, and $\tilde{\Omega} = -30$ dB. Fig. 6 indicates clearly that the SER of the system significantly depends on the distances d_{SR} and d_{RD} . For the variable gain relaying, the system performance is the best when $d_{SR} = d_{RD} = 0.5$ while that for fixed gain relaying is when $d_{SR} = 0.7$ and $d_{RD} = 0.3$. Furthermore, when $d_{SR} = 0.3$ and $d_{RD} = 0.7$ the difference between the SERs of fixed gain relaying and variable gain relaying is the largest in three considered cases. In the case of $d_{SR} = 0.7, d_{RD} = 0.3$ the difference is smallest. Therefore, depending on the case of fixed or variable gain relaying is applied to select the suitable distances between three nodes, better performance can be obtained. On the other hand, when the summation of the distances is a constant, the optimal values of d_{SR} and d_{RD} in the cases of fixed and variable gain relaying are available. Thus, in the next figure, we will investigate the optimal distance for this system.

In Fig. 7, we study the impact of the distance d_{SR} on the SER of the considered FD-V2V communication system. We evaluate the SERs with $d_{SR} + d_{RD} = 1$ for three cases of SNR i.e. SNR = 10, 20, 30 dB. It is obvious that the optimal values of d_{SR} for the case of fixed gain and variable gain are different. For the

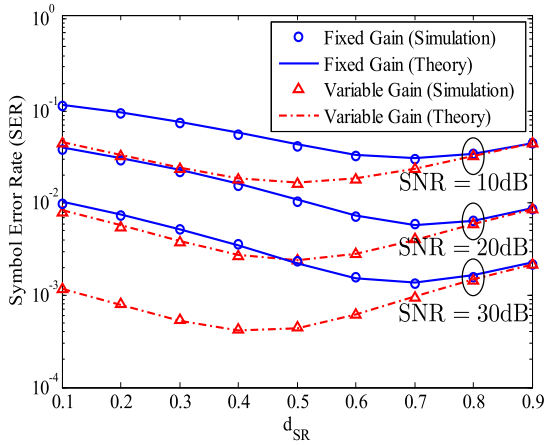


Fig. 7. The SERs of the considered system versus the distance d_{SR} for different average SNRs.

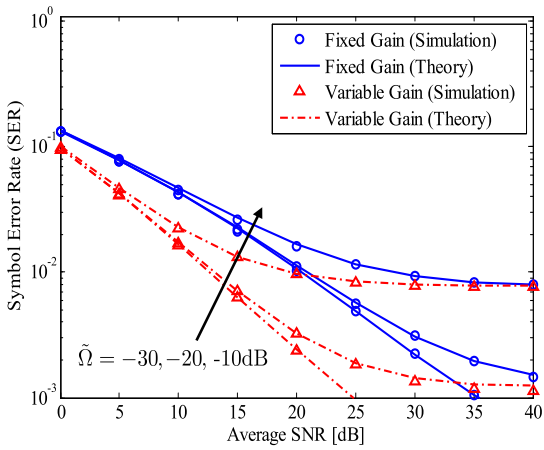


Fig. 8. The impact of RSI on SER of the considered FD-V2V communication system with $d_{SR} = d_{RD} = 0.5$, $\alpha = 4$.

case of fixed gain relaying, the optimal distances are $d_{SR} = 0.7$ and $d_{RD} = 0.3$ for three considered cases of SNR. For the case of variable gain relaying, the optimal distances depends on the average SNR. When SNR = 10, 20 dB, the optimal distances are $d_{SR} = d_{RD} = 0.5$. However, when SNR = 30 dB, the optimal distances are $d_{SR} = 0.4$ and $d_{RD} = 0.6$.

Finally, Fig. 8 illustrates the impact of the RSI on the SER of the system with $d_{SR} = d_{RD} = 0.5$, $\alpha = 4$. This figure represents the importance of SIC capability on the FD system. In the case of small RSI, such as $\tilde{\Omega} = -30$ dB, the SERs continuously go down when SNR increases. However, when the RSI is stronger, such as $\tilde{\Omega} = -20$, -10 dB the SERs go down slowly and reach the error floor faster. For the case of variable gain relaying, the SER reach the error floor at SNR = 30 dB when $\tilde{\Omega} = -20$ dB and at SNR = 20 dB when $\tilde{\Omega} = -10$ dB. We can also see that the SER of variable gain relaying is lower than those of fixed gain relaying, not only in Fig. 8 but also in other figures.

5. Conclusion

The FD-V2V communication system which combines the FD technique and the V2V communication is a promising system for the future wireless networks. In this paper, we studied the outage probability and symbol error rate of this system where the relay operates in FD mode and uses amplify-and-forward protocol. We also investigated the cases of fixed gain and variable gain at the relay node. Firstly, we successfully derived the expressions of the

outage probability and symbol error rate in two cases over double Rayleigh fading channels. Then, we analyzed the system performance in comparison with this system over Rayleigh fading channel. The numerical results showed that when the system operate in V2V communication over double Rayleigh fading channels, the system performance strongly degrades compared with that over Rayleigh fading channel for both cases of fixed and variable gain relaying. Furthermore, the impact of the distances, path loss exponent, and the residual self-interference also examined. On the other hand, we found the optimal values of the distances for both cases of fixed and variable gain relaying. Based on these results, we can apply various methods such as using suitable distances between vehicles in FD-V2V communication system to achieve the best performance. In the near future, we will extend our work by analyzing the scenario where the interference is considered as useful signal for V2V communication systems.

Declaration of Competing Interest

The authors declare that they have no known competing financial interests or personal relationships that could have appeared to influence the work reported in this paper.

Appendix A

This appendix provides the step-by-step derivations, showing how to obtain the outage probabilities in the case of fixed and variable gain of the considered FD-V2V communication system over double Rayleigh fading channels.

Firstly, we start with the Rayleigh fading channel. The probability density function (PDF) and cumulative distribution function (CDF) of the instantaneous channel gain $\rho = |g|^2$ are respectively given by

$$f_{\rho}(x) = \frac{1}{\Omega} \exp\left(-\frac{x}{\Omega}\right) \quad (16)$$

$$F_{\rho}(x) = 1 - \exp\left(-\frac{x}{\Omega}\right), \quad (17)$$

where $\Omega = \mathbb{E}\{\rho\}$.

For the double Rayleigh fading channels in V2V communications, the instantaneous channel gain $|h|^2$ is considered as the multiplication of two independent variables $|g_1|^2$ and $|g_2|^2$, where $|g_1|^2$ and $|g_2|^2$ are the instantaneous channel gains of the Rayleigh fading channel. Therefore, $|h|^2 = |g_1|^2 |g_2|^2 = \rho_1 \rho_2$. Due to the fact that ρ_1 and ρ_2 are independent variables, thus we have the CDF of $|h|^2$ as

$$\begin{aligned} F_{|h|^2}(x) &= \Pr(\rho_1 \rho_2 \leq x) \\ &= \int_0^{\infty} \Pr\left(\rho_2 \leq \frac{x}{\rho_1}\right) f_{\rho_1}(y) dy \\ &= 1 - \frac{1}{\Omega_1} \int_0^{\infty} \exp\left(-\frac{y}{\Omega_1} - \frac{x}{y\Omega_2}\right) dy \\ &= 1 - \sqrt{\frac{4x}{\Omega_1 \Omega_2}} K_1\left(\sqrt{\frac{4x}{\Omega_1 \Omega_2}}\right). \end{aligned} \quad (18)$$

From (18), we can obtain the PDF of $|h|^2$ as

$$f_{|h|^2}(x) = \frac{2}{\Omega_1 \Omega_2} K_0\left(\sqrt{\frac{4x}{\Omega_1 \Omega_2}}\right), \quad (19)$$

where $\Omega_1 = \mathbb{E}\{\rho_1\}$, $\Omega_2 = \mathbb{E}\{\rho_2\}$. As can be seen from (18), the double Rayleigh fading remarkably increases the computation complexity compared with (17) of the Rayleigh fading. On the other hand, the PDF and CDF of $|h|^2$ implicitly take into account the effects of scatterers around the transmitter and the receiver which include the fluctuating amplitude and phase of the signals, the Doppler shifts caused by the movement of vehicles [39].

It is noted that, from (10), we have

$$P_{\text{out}}^f = \Pr\{\gamma_f < x\} = \Pr\left\{\frac{(d_{\text{SR}}d_{\text{RD}})^{-\alpha} P_S P_R X Y}{d_{\text{RD}}^{-\alpha} P_R Y (\gamma_{\text{RSI}} + \sigma^2) + \sigma^2 / G_f^2} < x\right\}, \quad (20)$$

$$P_{\text{out}}^v = \Pr\{\gamma_v < x\} = \Pr\left\{\frac{(d_{\text{SR}}d_{\text{RD}})^{-\alpha} P_S P_R X Y}{d_{\text{RD}}^{-\alpha} P_R Y (\gamma_{\text{RSI}} + \sigma^2) + \sigma^2 (d_{\text{SR}}^{-\alpha} P_S X + \gamma_{\text{RSI}} + \sigma^2)} < x\right\}, \quad (21)$$

where $X = \rho_1 \rho_2$; $Y = \rho_3 \rho_4$.

Combining with the PDF and CDF of the instantaneous channel gain of double Rayleigh fading channels which are given in (18) and (19), we can calculate the P_{out}^f and P_{out}^v of the system as shown on the top of next page.

For the P_{out}^f , from (20), we derive (22). It is also noted that since X and Y (which are presented in Section 3) are the double Rayleigh fading channels, the PDF and CDF of X and Y are given in (18) and (19). Therefore, the P_{out}^f is calculated as in (23). To resolve the integral in (23), we set $e^{-\xi} = \nu$, thus (23) becomes (24). Applying the Gaussian-Chebyshev quadrature method in [40], we obtain the OP in the case of fixed gain relaying as in (11).

$$P_{\text{out}}^f = \Pr\left\{\frac{(d_{\text{SR}}d_{\text{RD}})^{-\alpha} P_S P_R X Y}{d_{\text{RD}}^{-\alpha} P_R Y (\gamma_{\text{RSI}} + \sigma^2) + \sigma^2 / G_f^2} < x\right\} = \Pr\left\{X < \frac{\sigma^2 x}{G_f^2 (d_{\text{SR}}d_{\text{RD}})^{-\alpha} P_S P_R Y} + \frac{(\gamma_{\text{RSI}} + \sigma^2)x}{d_{\text{SR}}^{-\alpha} P_S}\right\} = 1 - \int_0^\infty \left[1 - F_X\left(\frac{\sigma^2 x}{G_f^2 (d_{\text{SR}}d_{\text{RD}})^{-\alpha} P_S P_R \xi} + \frac{(\gamma_{\text{RSI}} + \sigma^2)x}{d_{\text{SR}}^{-\alpha} P_S}\right)\right] f_Y(\xi) d\xi \quad (22)$$

$$P_{\text{out}}^f = 1 - \int_0^\infty \sqrt{\frac{4\sigma^2 x}{\Omega_1 \Omega_2 G_f^2 (d_{\text{SR}}d_{\text{RD}})^{-\alpha} P_S P_R \xi} + \frac{4(\gamma_{\text{RSI}} + \sigma^2)x}{\Omega_1 \Omega_2 d_{\text{SR}}^{-\alpha} P_S}} \times K_1\left(\sqrt{\frac{4\sigma^2 x}{\Omega_1 \Omega_2 G_f^2 (d_{\text{SR}}d_{\text{RD}})^{-\alpha} P_S P_R \xi} + \frac{4(\gamma_{\text{RSI}} + \sigma^2)x}{\Omega_1 \Omega_2 d_{\text{SR}}^{-\alpha} P_S}}\right) \times \frac{2}{\Omega_3 \Omega_4} K_0\left(\sqrt{\frac{4\xi}{\Omega_3 \Omega_4}}\right) d\xi = 1 - C_f \int_0^\infty \sqrt{\frac{A_f x}{\xi} + B_f x} K_1\left(\sqrt{\frac{A_f x}{\xi} + B_f x}\right) K_0(\sqrt{2C_f \xi}) d\xi \quad (23)$$

$$P_{\text{out}}^f = 1 - C_f \int_0^1 \sqrt{\frac{A_f x}{-\ln \nu} + B_f x} K_1\left(\sqrt{\frac{A_f x}{-\ln \nu} + B_f x}\right) \times K_0(\sqrt{-2C_f \ln \nu}) \frac{d\nu}{\nu} \quad (24)$$

$$P_{\text{out}}^v = \Pr\left\{\frac{(d_{\text{SR}}d_{\text{RD}})^{-\alpha} P_S P_R X Y}{d_{\text{RD}}^{-\alpha} P_R Y (\gamma_{\text{RSI}} + \sigma^2) + \sigma^2 (d_{\text{SR}}^{-\alpha} P_S X + \gamma_{\text{RSI}} + \sigma^2)} < x\right\} = \Pr\{d_{\text{SR}}^{-\alpha} P_S X (d_{\text{RD}}^{-\alpha} P_R Y - \sigma^2 x) < d_{\text{RD}}^{-\alpha} P_R Y (\gamma_{\text{RSI}} + \sigma^2) x + (\gamma_{\text{RSI}} + \sigma^2) \sigma^2 x\} \quad (25)$$

$$P_{\text{out}}^v = \Pr\left\{(d_{\text{SR}}d_{\text{RD}})^{-\alpha} P_S P_R X Z < d_{\text{RD}}^{-\alpha} P_R \left(Z + \frac{\sigma^2 x}{d_{\text{RD}}^{-\alpha} P_R}\right) (\gamma_{\text{RSI}} + \sigma^2) x + (\gamma_{\text{RSI}} + \sigma^2) \sigma^2 x\right\} \quad (26)$$

$$P_{\text{out}}^v = 1 - \int_0^\infty \left[1 - F_X\left(\frac{(\gamma_{\text{RSI}} + \sigma^2) \sigma^2 (x + x^2)}{(d_{\text{SR}}d_{\text{RD}})^{-\alpha} P_S P_R \xi} + \frac{(\gamma_{\text{RSI}} + \sigma^2) x}{d_{\text{SR}}^{-\alpha} P_S}\right)\right] \times f_Z\left(\xi + \frac{\sigma^2 x}{d_{\text{RD}}^{-\alpha} P_R}\right) d\xi = 1 - \int_0^\infty \sqrt{\frac{4(\gamma_{\text{RSI}} + \sigma^2) \sigma^2 (x + x^2)}{\Omega_1 \Omega_2 (d_{\text{SR}}d_{\text{RD}})^{-\alpha} P_S P_R \xi} + \frac{4(\gamma_{\text{RSI}} + \sigma^2) x}{\Omega_1 \Omega_2 d_{\text{SR}}^{-\alpha} P_S}} \times K_1\left(\sqrt{\frac{4(\gamma_{\text{RSI}} + \sigma^2) \sigma^2 (x + x^2)}{\Omega_1 \Omega_2 (d_{\text{SR}}d_{\text{RD}})^{-\alpha} P_S P_R \xi} + \frac{4(\gamma_{\text{RSI}} + \sigma^2) x}{\Omega_1 \Omega_2 d_{\text{SR}}^{-\alpha} P_S}}\right) \times \frac{2}{\Omega_3 \Omega_4} K_0\left(\sqrt{\frac{4(\xi + \frac{\sigma^2 x}{d_{\text{RD}}^{-\alpha} P_R})}{\Omega_3 \Omega_4}}\right) d\xi = 1 - C_v \int_0^\infty \sqrt{\frac{A_v (x + x^2)}{\xi} + B_v x} K_1\left(\sqrt{\frac{A_v (x + x^2)}{\xi} + B_v x}\right) \times K_0(\sqrt{2C_v \xi} + D_v x) d\xi \quad (27)$$

$$P_{\text{out}}^v = 1 - C_v \int_0^1 \sqrt{\frac{A_v (x + x^2)}{-\ln \nu} + B_v x} K_1\left(\sqrt{\frac{A_v (x + x^2)}{-\ln \nu} + B_v x}\right) \times K_0(\sqrt{2C_v (-\ln \nu)} + D_v x) \frac{d\nu}{\nu} \quad (28)$$

For the P_{out}^v , from (21), we calculate the OP of the system in this case (i.e. the variable gain relaying) as in (25). Then, by setting $Y = Z + \frac{\sigma^2 x}{d_{\text{RD}}^{-\alpha} P_R}$, (25) becomes (26). From (26), we can calculate the P_{out}^v by using the same method as for P_{out}^f . After some mathematical transforms, which are combined with the Gaussian-Chebyshev quadrature method in [40], (28) becomes (12). The proof of Appendix A is complete.

Appendix B

This appendix presents detailed derivations to obtain the SER_f and SER_v of the considered FD-V2V communication system.

From (13), after some mathematical transforms, the SER can be rewritten as

$$\text{SER} = \frac{a\sqrt{b}}{2\sqrt{2\pi}} \int_0^\infty \frac{e^{-bx/2}}{\sqrt{x}} F(x) dx. \quad (29)$$

Then, we substitute $F(x)$ in (29) by P_{out}^f in (11) to obtain SER_f and by P_{out}^v in (12) to obtain SER_v .

$$\begin{aligned}
SER_f &= \frac{a\sqrt{b}}{2\sqrt{2\pi}} \left[\int_0^\infty \frac{e^{-bx/2}}{\sqrt{x}} dx - \int_0^\infty \frac{e^{-bx/2}}{\sqrt{x}} \frac{\pi C_f}{2M} \sum_{m=1}^M \frac{\sqrt{1-\phi_m^2}}{z} \right. \\
&\quad \left. \times \sqrt{\frac{A_f x}{-\ln z}} + B_f x K_0(\sqrt{-2C_f \ln z}) K_1 \left(\sqrt{\frac{A_f x}{-\ln z}} + B_f x \right) dx \right] \\
&= \frac{a\sqrt{b}}{2\sqrt{2\pi}} \left[\int_0^\infty \frac{e^{-bx/2}}{\sqrt{x}} dx - \frac{\pi C_f}{2M} \sum_{m=1}^M \frac{\sqrt{1-\phi_m^2}}{z} \sqrt{\frac{A_f}{-\ln z}} + B_f \right. \\
&\quad \left. \times K_0(\sqrt{-2C_f \ln z}) \int_0^\infty e^{-bx/2} K_1 \left(\sqrt{\frac{A_f x}{-\ln z}} + B_f x \right) dx \right] \quad (30)
\end{aligned}$$

For the SER_f , we have (30) after some mathematical transforms. To derive the closed-form for the first integral in (30), we use [37, Eq.3.361.2] to have

$$\int_0^\infty \frac{e^{-bx/2}}{\sqrt{x}} dx = \sqrt{\frac{2\pi}{b}} \quad (31)$$

For the second integral in (30), we apply [37, Eq. 6.614.4] to have the result in (32). Then, we substitute (31) and (32) into (30) to obtain SER_f in (14).

$$\begin{aligned}
&\int_0^\infty e^{-bx/2} K_1 \left(\sqrt{\frac{A_f x}{-\ln z}} + B_f x \right) dx \\
&= \exp \left(\frac{1}{4b} \left(\frac{A_f}{-\ln z} + B_f \right) \right) \frac{\Gamma(\frac{3}{2})\Gamma(\frac{1}{2})}{\sqrt{\frac{b}{2} \left(\frac{A_f}{-\ln z} + B_f \right)}} \\
&\quad \times W_{-\frac{1}{2}, \frac{1}{2}} \left(\frac{1}{2b} \left(\frac{A_f}{-\ln z} + B_f \right) \right) \quad (32)
\end{aligned}$$

Similar to the SER_f , the SER_v is calculated in (33). To derive the closed-form expression for the second integral in (33), we change the variable by setting $\chi = e^{-bx/2}$, thus $x = -\frac{2}{b} \ln \chi$, and can rewrite the second integral as in (34).

$$\begin{aligned}
SER_v &= \frac{a\sqrt{b}}{2\sqrt{2\pi}} \left[\int_0^\infty \frac{e^{-bx/2}}{\sqrt{x}} dx - \int_0^\infty \frac{e^{-bx/2}}{\sqrt{x}} \frac{\pi C_v}{2M} \sum_{m=1}^M \frac{\sqrt{1-\phi_m^2}}{z} \right. \\
&\quad \times \sqrt{\frac{A_v(x^2+x)}{-\ln z}} + B_v x K_0(\sqrt{-2C_v \ln z + D_v x}) \\
&\quad \left. \times K_1 \left(\sqrt{\frac{A_v(x^2+x)}{-\ln z}} + B_v x \right) dx \right] \\
&= \frac{a\sqrt{b}}{2\sqrt{2\pi}} \left[\int_0^\infty \frac{e^{-bx/2}}{\sqrt{x}} dx - \frac{\pi C_v}{2M} \sum_{m=1}^M \frac{\sqrt{1-\phi_m^2}}{z} \int_0^\infty \right. \\
&\quad \times e^{-bx/2} \sqrt{\frac{A_v(x+1)}{-\ln z}} + B_v x K_0(\sqrt{-2C_v \ln z + D_v x}) \\
&\quad \left. \times K_1 \left(\sqrt{\frac{A_v(x^2+x)}{-\ln z}} + B_v x \right) dx \right] \quad (33) \\
&\int_0^\infty e^{-bx/2} \sqrt{\frac{A_v(x+1)}{-\ln z}} + B_v x K_0(\sqrt{-2C_v \ln z + D_v x}) \\
&\quad \times K_1 \left(\sqrt{\frac{A_v(x^2+x)}{-\ln z}} + B_v x \right) dx
\end{aligned}$$

$$\begin{aligned}
&= \frac{2}{b} \int_0^1 \sqrt{\frac{A_v(b-2\ln \chi)}{-b \ln z}} + B_v x K_0 \left(\sqrt{-2C_v \ln z - \frac{2D_v \ln \chi}{b}} \right) \\
&\quad \times K_1 \left(\sqrt{-\frac{2}{b} \left[\frac{A_v(b-2\ln \chi)}{-b \ln z} + B_v \right] \ln \chi} \right) d\chi \quad (34)
\end{aligned}$$

Then, using the Gaussian-Chebyshev quadrature method in [40] to derive the closed-form for the integral in (34). After that, we combine this with (31) to obtain SER_v in (15). The proof is complete.

References

- [1] F.-L. Luo, C. Zhang, Signal Processing for 5G: Algorithms and Implementations, John Wiley & Sons, 2016.
- [2] Q.C. Li, H. Niu, A.T. Papathanassiou, G. Wu, 5g network capacity: key elements and technologies, IEEE Veh. Technol. Mag. 9 (1) (2014) 71–78.
- [3] Y. Alsaba, C.Y. Leow, S.K.A. Rahim, Full-duplex cooperative non-orthogonal multiple access with beamforming and energy harvesting, in: IEEE Access, vol. 6, 2018, pp. 19 726–19 738.
- [4] D. Bharadia, E. McMillin, S. Katti, Full duplex radios, in: ACM SIGCOMM Computer Communication Review, vol. 43, issue 4, ACM, 2013, pp. 375–386.
- [5] A. Sabharwal, P. Schniter, D. Guo, D.W. Bliss, S. Rangarajan, R. Wichman, In-band full-duplex wireless: challenges and opportunities, IEEE J. Sel. Areas Commun. 32 (9) (2014) 1637–1652.
- [6] X. Li, C. Tepedelenlioglu, H. Senol, Channel estimation for residual self-interference in full duplex amplify-and-forward two-way relays, IEEE Trans. Wirel. Commun. 99 (2017) 1.
- [7] E. Antonio-Rodríguez, R. López-Valcarce, T. Riihonen, S. Werner, R. Wichman, Adaptive self-interference cancellation in wideband full-duplex decode-and-forward MIMO relays, in: 2013 IEEE 14th Workshop on Signal Processing Advances in Wireless Communications, SPAWC, IEEE, 2013, pp. 370–374.
- [8] O. Abbasi, A. Ebrahimi, Cooperative NOMA with full-duplex amplify-and-forward relaying, Transp. Emerg. Telecommun. Technol. 29 (7) (2018) e3421.
- [9] B.C. Nguyen, X.N. Tran, D.T. Tran, Performance analysis of in-band full-duplex amplify-and-forward relay system with direct link, in: 2018 2nd International Conference on Recent Advances in Signal Processing, Telecommunications & Computing, SigTelCom, IEEE, 2018, pp. 192–197.
- [10] B.C. Nguyen, T.M. Hoang, P.T. Tran, Performance analysis of full-duplex decode-and-forward relay system with energy harvesting over Nakagami-m fading channels, AEÜ, Int. J. Electron. Commun. 98 (2019) 114–122.
- [11] T.M. Hoang, V. Van Son, N.C. Dinh, P.T. Hiep, Optimizing duration of energy harvesting for downlink NOMA full-duplex over Nakagami-m fading channel, AEÜ, Int. J. Electron. Commun. (2018).
- [12] A. Zanella, A. Bazzi, B.M. Masini, Relay selection analysis for an opportunistic two-hop multi-user system in a Poisson field of nodes, IEEE Trans. Wirel. Commun. 16 (2) (2016) 1281–1293.
- [13] C. La Palombara, V. Tralli, B.M. Masini, A. Conti, Relay-assisted diversity communications, IEEE Trans. Veh. Technol. 62 (1) (2012) 415–421.
- [14] X.N. Tran, B.C. Nguyen, D.T. Tran, Outage probability of two-way full-duplex relay system with hardware impairments, in: 2019 3rd International Conference on Recent Advances in Signal Processing, Telecommunications & Computing, SigTelCom, IEEE, 2019, pp. 135–139.
- [15] G.J. Gonzalez, F.H. Gregorio, J.E. Cousseau, T. Riihonen, R. Wichman, Full-duplex amplify-and-forward relays with optimized transmission power under imperfect transceiver electronics, EURASIP J. Wirel. Commun. Netw. (2017).
- [16] G. Naik, B. Choudhury, et al., IEEE 802.11 bd & 5g nr v2x: evolution of radio access technologies for v2x communications, arXiv preprint, arXiv:1903.08391, 2019.
- [17] A. Nabil, K. Kaur, C. Dietrich, V. Marojevic, Performance analysis of sensing-based semi-persistent scheduling in c-v2x networks, in: 2018 IEEE 88th Vehicular Technology Conference, VTC-Fall, IEEE, 2019, pp. 1–5.
- [18] S. Biswas, R. Tatchikou, F. Dion, Vehicle-to-vehicle wireless communication protocols for enhancing highway traffic safety, IEEE Commun. Mag. 44 (1) (2006) 74–82.
- [19] C. Campolo, A. Molinaro, A.O. Berthet, A. Vinel, Full-duplex radios for vehicular communications, IEEE Commun. Mag. 55 (6) (2017) 182–189.
- [20] Y. Ai, M. Cheffena, A. Mathur, H. Lei, On physical layer security of double Rayleigh fading channels for vehicular communications, IEEE Wirel. Commun. Lett. 7 (6) (2018) 1038–1041.
- [21] A.S. Akki, F. Haber, A statistical model of mobile-to-mobile land communication channel, IEEE Trans. Veh. Technol. 35 (1) (1986) 2–7.
- [22] I.Z. Kovacs, Radio Channel Characterisation for Private Mobile Radio Systems-Mobile-to-Mobile Radio Link Investigations, Ph.D. dissertation, Aalborg University, 2002.
- [23] V. Erceg, S.J. Fortune, J. Ling, A. Rustako, R.A. Valenzuela, Comparisons of a computer-based propagation prediction tool with experimental data collected in urban microcellular environments, IEEE J. Sel. Areas Commun. 15 (4) (1997) 677–684.

- [24] D. Chizhik, J. Ling, P.W. Wolniansky, R.A. Valenzuela, N. Costa, K. Huber, Multiple-input-multiple-output measurements and modeling in Manhattan, *IEEE J. Sel. Areas Commun.* 21 (3) (April 2003) 321–331.
- [25] J. Wu, C. Xiao, Performance analysis of wireless systems with doubly selective Rayleigh fading, *IEEE Trans. Veh. Technol.* 56 (2) (2007) 721–730.
- [26] M. Seyfi, S. Muhaidat, J. Liang, M. Uysal, Relay selection in dual-hop vehicular networks, *IEEE Signal Process. Lett.* 18 (2) (2011) 134–137.
- [27] Y. Chen, L. Wang, Y. Ai, B. Jiao, L. Hanzo, Performance analysis of NOMA-SM in vehicle-to-vehicle massive MIMO channels, *IEEE J. Sel. Areas Commun.* 35 (12) (2017) 2653–2666.
- [28] T.T. Duy, G.C. Alexandropoulos, V.T. Tung, V.N. Son, T.Q. Duong, Outage performance of cognitive cooperative networks with relay selection over double-Rayleigh fading channels, *IET Commun.* 10 (1) (2016) 57–64.
- [29] H. Lei, I.S. Ansari, G. Pan, B. Alomair, M.-S. Alouini, Secrecy capacity analysis over α - μ fading channels, *IEEE Commun. Lett.* 21 (6) (2017) 1445–1448.
- [30] A. Bazzi, C. Campolo, B.M. Masini, A. Molinaro, A. Zanella, A.O. Berthet, Enhancing cooperative driving in IEEE 802.11 vehicular networks through full-duplex radios, *IEEE Trans. Wirel. Commun.* 17 (4) (2018) 2402–2416.
- [31] C.-X. Mao, S. Gao, Y. Wang, Dual-band full-duplex Tx/Rx antennas for vehicular communications, *IEEE Trans. Veh. Technol.* 67 (5) (2018) 4059–4070.
- [32] M. Yang, S.-W. Jeon, D.K. Kim, Interference management for in-band full-duplex vehicular access networks, *IEEE Trans. Veh. Technol.* 67 (2) (2018) 1820–1824.
- [33] S. Hong, J. Brand, J.I. Choi, M. Jain, J. Mehlman, S. Katti, P. Levis, Applications of self-interference cancellation in 5G and beyond, *IEEE Commun. Mag.* 52 (2) (Feb. 2014) 114–121.
- [34] F. Jameel, S. Wyne, M.A. Javed, S. Zeadally, Interference-aided vehicular networks: future research opportunities and challenges, *IEEE Commun. Mag.* 56 (10) (2018) 36–42.
- [35] K. Yang, H. Cui, L. Song, Y. Li, Efficient full-duplex relaying with joint antenna-relay selection and self-interference suppression, *IEEE Trans. Wirel. Commun.* 14 (7) (Jul. 2015) 3991–4005.
- [36] A. Goldsmith, *Wireless Communications*, Cambridge University Press, 2005.
- [37] A. Jeffrey, D. Zwillinger, *Table of Integrals, Series, and Products*, Academic Press, 2007.
- [38] C. Li, Z. Chen, Y. Wang, Y. Yao, B. Xia, Outage analysis of the full-duplex decode-and-forward two-way relay system, *IEEE Trans. Veh. Technol.* 66 (5) (May 2017) 4073–4086.
- [39] I.Z. Kovacs, P.C.F. Eggers, K. Olesen, L.G. Petersen, Investigations of outdoor-to-indoor mobile-to-mobile radio communication channels, in: *Proceedings IEEE 56th Vehicular Technology Conference*, vol. 1, IEEE, 2002, pp. 430–434.
- [40] M. Abramowitz, I.A. Stegun, *Handbook of Mathematical Functions with Formulas, Graphs, and Mathematical Tables*, vol. 9, Dover, New York, 1972.